

The impacts of dew-induced foliar shielding on the energy, water and isotope balance of leaves

Cynthia Gerlein-Safdi¹, Craig James Sinkler^{2,3}, Kelly Krispin Caylor¹

¹ Princeton University, Dept. of Civil and Environmental Engineering, Princeton, NJ 08544, USA

² Rider University, Dept. of Geological, Environmental, and Marine Sciences, Lawrenceville, NJ 08648, USA

³ EarthRes Group, Inc., Pipersville, PA 18947, USA

Author for correspondence: *Cynthia Gerlein-Safdi*

Tel: +1-609-865-5428

Email: *cgerlein@princeton.edu*

For Cover Letter (3-4 sentences):

We hypothesize that the deposition of water droplets from dew or fog will block part of the energy incident on a leaf. The reduction of incoming energy induces a significant decrease in transpiration, which in turn affects leaf water status and leaf water isotopes. This study is the first one to experimentally quantify the impact of non-meteoric water deposition on leaf energy and water balance. We also present a new protocol for the rapid analysis of leaf samples using a laser spectrometer and an induction module. While foliar uptake of non-meteoric water is an important source of water for many ecosystems, this work challenges the interpretation of prior results that used leaf water isotopes to estimate contributions of non-meteoric uptake to total leaf water balance. Specifically, both our experimental results and subsequent modeling analysis suggest that the indirect energy balance effect of non-meteoric water on leaf water isotopes has a similar amplitude - but opposite sign - to the direct water balance effect of foliar uptake on leaf water isotopes.

Running head: Dew-induced foliar shielding in leaves

Name of two referees: Brent Helliker (editorial review board) and Lucas Cernusak.

Summary

The uptake of water from the surface of the leaves (foliar uptake) is common when rainfall is scarce and non-meteoric water (dew or fog) is the only water source. However, many species have hydrophobic leaves. Past studies have not differentiated between the uptake of water and the impact of the droplets on the energy balance of the leaf, which we call ‘foliar shielding’. Leaves of the hydrophobic *Colocasia esculenta* are sprayed with isotopically enriched water. We develop a protocol using a laser spectrometer and an induction module for the rapid analysis of leaf samples. The leaf water potential and water isotopes are monitored for different water-stress conditions and their spatial pattern predicted using the Farquhar-Gan model. Dew-treated leaves exhibit a higher water potential ($P < 0.05$) and c. 30% decrease in transpiration rate ($P < 0.001$) compared to the control. Dew treated leaves also have a depleted water isotopic composition compared to the control ($P < 0.001$). Three possible mechanisms are proposed for the interaction of water droplets with the leaf energy balance. Comparing previous studies on foliar uptake to our results, we conclude that foliar shielding has a comparable yet opposite effect to foliar uptake on leaf water isotopes.

Key words: *Colocasia esculenta*, dew, Farquhar-Gan model, fog, foliar uptake, foliar shielding, induction module, laser spectrometer, leaf energy balance, leaf water isotopes

¹ I. Introduction

² Non-meteoric water (dew or fog) is an important source of water for many plants that occurs consist-
³ently in all environments. Observations of plants using dew [Yates and Hutley, 1995, Andrade, 2003,
⁴ Lakatos et al., 2012, Berkelhammer et al., 2013] or fog water [Stanton and Horn, 2013, Eller et al., 2013,
⁵ Berry and Smith, 2014] through foliar uptake have focused on the particular circumstances in which plants
⁶ conduct foliar uptake of condensed water and the impact of these subsidies on water balance. In some cases,
⁷ vegetation in dry and fog-prone areas such as coastlands [Burgess and Dawson, 2004, Limm and Dawson, 2010,
⁸ Stanton and Horn, 2013] or mountain hillsides [Berry et al., 2014a] have adapted to using fog as their main
⁹ source of water. Similarly, dew water can be a major source of water on islands where fresh water is scarce
¹⁰ [Clus et al., 2008]. In addition, some plants which lack access to soil water - including epiphytic bromeliads
¹¹ [Andrade, 2003, Gotsch et al., 2015] and lichens [Lakatos et al., 2012] - have physical features allowing them
¹² to collect dew water. The exact mechanism of foliar uptake is still in debate, but is commonly thought to occur
¹³ through the leaf cuticles [Yates and Hutley, 1995, Schreiber and Schönher, 2009, Limm and Dawson, 2010,
¹⁴ Eller et al., 2013]. Recent evidence also points towards the water entering the leaf at the junction between the
¹⁵ petiole and the stem, in particular in conifers [T. Dawson, private communication].

¹⁶ While non-meteoric water uptake is of interest as a potential leaf water subsidy, it is also well-known
¹⁷ that most species have water-repellent leaves [Neinhuis and Barthlott, 1997] that are not adapted to take up
¹⁸ water. For most plants, non-meteoric water deposition is a potential nuisance: in cold climates it may freeze
¹⁹ and cause damage to the leaf [Jordan and Smith, 1994], while in warm environments it may cause rotting
²⁰ and facilitate pathogen infection [Evans et al., 1992]. Indeed, leaves that are repeatedly exposed to dew have
²¹ even been shown to become more water-repellent [Aryal and Neuner, 2009]. However, during dew and fog
²² events, micro-droplets of water will indeed form on the surface of even very hydrophobic leaves because of
²³ the influence of leaf surface properties on contact angle hysteresis [Gao and McCarthy, 2006, Holder, 2012].

²⁴ Given the ubiquity of dew and fog events across ecosystems, our goal is to broaden the scope of inquiry
²⁵ related to non-meteoric water and its interaction with the energy and water balance of plant leaves and

26 canopies. Firstly, we assess the potential for condensed water on the surface of leaves to directly alter
27 leaf energy balance. Secondly, we examine the indirect effect of non-meteoric water's energy subsidies on
28 subsequent leaf water use and leaf water balance, particularly during periods of extreme water stress. Finally,
29 we explore how these direct energy balance and indirect water balance effects combine to alter the isotopic
30 composition of leaves exposed to non-meteoric water, even in settings where foliar uptake is negligible.

31 **Leaf energy balance** — *[THIS NEEDS TO BE FLESHED OUT A BIT MORE. MORE DETAIL ABOUT*
32 *THE ENERGY BALANCE TERMS, MAYBE SOME EQS, ETC...?]* Because they are subject to high radiative
33 fluxes and have low thermal mass, leaves can often be warmer than the surrounding air. The leaf temperature
34 will in turn affect the saturation vapor pressure, isotope fractionation, transpiration, and photosynthesis.
35 Smaller leaves tend to be at a temperature closer to the ambient air, since their boundary layer is thinner.
36 This is the reason why, on a single tree, leaves exposed to the sun are usually smaller than shaded ones. To
37 stay cool, leaves use a combination of re-radiation (transfer of energy to the surroundings), convection (heat
38 loss as cool air moves over the surface of the leaf) and evaporative cooling (evaporation of water inside the
39 leaf into water vapor, which is an exothermic process) [Gates, 1980, Vogel, 2012]. During a drought, leaves
40 must preserve water to maintain turgor pressure, which competes with evaporative cooling. In the absence
41 of evaporative cooling, leaves must balance energy inputs via re-radiation and convection. For large leaves,
42 and during periods of low wind speed, these mechanisms are often insufficient to maintain a temperature
43 commensurate with efficient leaf function. If periods of high leaf temperature persist, drought conditions lead
44 to leaf shedding, and - eventually - plant mortality.

45 Non-meteoric water supplies a pool of water whose subsequent evaporation provides a form of externalized
46 evaporative cooling that can supplement scarce leaf water. While dew deposition is often a modest 0.5
47 mm/day [Monteith, 1963, Clus et al., 2008], values as high at 0.8 mm/day have been reported in tropical
48 forests [Andrade, 2003, Lakatos et al., 2012]. A daily deposition rate of *[XX]* corresponds to only 1/6 of
49 daily potential transpiration in tropical areas and even less in arid climates [Monteith, 1963], suggesting that
50 water savings provided by foliar shielding are limited. However, the presence of droplets increases leaf albedo

51 [Pinter, 1986], as well as surface roughness [Defraeye et al., 2013]. These changes in albedo and roughness
52 lead to less energy absorption and a deeper leaf boundary layer respectively, which serve to decrease vapor
53 pressure deficits (VPDs) and lower evaporative demand. Shifts in surface roughness have been used to explain
54 fog-induced suppression of nighttime respiration in redwoods [Limm et al., 2009].

55 Foliar shielding directly affects leaf energy balance, with indirect effects on leaf water balance. Depending
56 on temperature and relative humidity, dew formed during pre-dawn conditions can persist from c. 1.5
57 [Abtew and Melesse, 2012] to 6 hours [Monteith, 1957] after sunrise. Dew and fog can also form in the late
58 afternoon before sunset [Wilson et al., 1999, Kabela et al., 2009]. Although neither dew nor fog is usually
59 present at the hottest hour of the day, either can effectively shorten the duration of the water-stressed part of
60 the day. The energy subsidies provided by foliar shielding may be significant for the maintenance of leaf
61 water status during a period of soil water scarcity [Madeira et al., 2002, Proctor, 2012].

62 Although dew formation is usually included in global climate models (GCMs) [Rosenzweig and Abramopoulos, 1997],
63 the interaction of dew with vegetation energy and water balance is not commonly taken into account. Non-
64 meteoric water deposition events occur around the world, even in dryland ecosystems [Agam and Berliner, 2006],
65 and may affect large areas at the same time. Small changes in the energy, water, and carbon balance of
66 each single leaf can lead to large cumulative impacts at the ecosystem level. *TIGHTEN THIS ARGUMENT:*
67 *MAKE IT ABOUT SHIFTS IN DEW FREQUENCY, OR ???:* Including the interactions into GCMs would
68 allow modelers to better understand the response of vegetation to climate change and the feedback on CO₂
69 atmospheric concentrations.

70 **Leaf water isotopes** — The signature of foliar shielding on leaf energy and water balance should be
71 present in the leaf water isotopes of leaves strongly affected by non-meteoric water. In particular, decreasing
72 leaf transpiration caused by improved leaf energy balance should lead to leaf water depletion in heavy isotopes
73 [Farquhar et al., 2006, Cernusak and Kahmen, 2013]. The balance of the stable isotopologues of water has
74 been used for decades to understand plant water fluxes [Allison et al., 1985, Ehleringer and Dawson, 1992,
75 Werner et al., 2012], but as the number of water sources and sinks increases, the interpretation of isotope data

76 can become difficult. The effect of foliar shielding on leaf water isotopes is, for example, likely to be opposite
77 to that of foliar uptake of isotopically heavy fog or dew [Scholl et al., 2010], which will enrich leaf water in
78 heavy isotopes. However, foliar uptake studies have so far not taken foliar shielding into account, even though
79 it likely results in an underestimation of the amount of water taken up by the leaf.

80 While the potential of surface droplets to alter leaf energy balance has been mentioned in previous work
81 [Limm et al., 2009, Berkelhammer et al., 2013], our study is the first to quantify the impacts of non-meteoric
82 water on coupled leaf water and energy balance.

83 Prior examinations of non-meteoric water have generally neglected the potential effects of condensed
84 water on leaf and canopy energy balance.

85 To address this gap, we present a study that focuses on the effect of non-meteoric water droplets on the
86 leaf energy balance, which we call ‘foliar shielding’.

87 In this study, we present three experiments that focus on the effects of water droplets deposition at the
88 surface of *Colocasia esculenta* leaves. This species is native to South East Asian tropical forests but has
89 been cultivated across the world for many centuries under the name of taro. With a contact angle of $\sim 164^\circ$
90 [Neinhuis and Barthlott, 1997], *Colocasia esculenta* is considered to have highly water-repellent leaves. Its
91 leaves can reach a size of up to c. 50 cm in length and c. 40 cm in width. We present the first protocol for the
92 fast analysis of small sized leaf samples, allowing for spatial and temporal high-resolution mapping of the
93 leaf-water properties. Using isotopically-labelled water as well as traditional plant physiology techniques, we
94 confirm that the *Colocasia esculenta* leaves do not uptake water from the surface of the leaves. So far, few
95 studies have attempted to map leaf isotopes because it is both time and labor intensive. While the number
96 of replicas presented in this study was limited by the novelty of the protocol, c. 550 plant samples were
97 analyzed. This number exceeds by a factor of [XX] the total number of samples analyzed by previous studies
98 that focused on spatial patterns of leaf water isotopes [Gan et al., 2002, Šantrůček et al., 2007]. We analyze
99 the spatial patterns of leaf water isotopic enrichment and compare them to three different models. In addition,
100 we show that foliar shielding decreases leaf transpiration and increases water potential, and we present

¹⁰¹ three mechanisms that explain the influence of water droplet deposition on the energy and water cycles of
¹⁰² water-repellent leaves. Finally, we compare our results to multiple foliar uptake studies. We conclude that
¹⁰³ foliar shielding has an opposite and larger effect on leaf isotopes than foliar uptake. It is therefore crucial to
¹⁰⁴ include foliar shielding in leaf isotope models to properly interpret isotope data of foliar uptake.

¹⁰⁵ **II. Materials and Methods**

¹⁰⁶ **II.1 The added value of stable isotopes**

¹⁰⁷ Stable isotopes of water hold great potential for resolving transpiration and evaporation fluxes across multiple
¹⁰⁸ scales [Griffis et al., 2010, Rothfuss et al., 2012, Wang et al., 2013]. The process of evaporation is accompa-
¹⁰⁹ nied by a high degree of isotopic fractionation that leads to evaporated water with an isotopic composition
¹¹⁰ depleted in the heavy isotopologues $H_2^{18}O$ and $HD^{16}O$. This is due to the difference in vapor pressure of the
¹¹¹ different isotopologues [Farquhar et al., 2006]. Isotopic compositions are commonly expressed in terms of
¹¹² the relative ratios

$$\delta_i = \left(\frac{R_i}{R_{r_i}} - 1 \right) \times 10^3 \quad (1)$$

¹¹³ of isotope ratios [Mook, 2006], where δ_i is expressed in ‰, and the index i stands for either ^{18}O or D.
¹¹⁴ $R_{^{18}O} = [H_2^{18}O]/[H_2^{16}O]$ and $R_D = [HD^{16}O]/[H_2^{16}O]$ are the isotope ratios, while the R_{r_i} are the ratios of
¹¹⁵ the corresponding reference standard. For water, the reference is the Vienna Standard Mean Ocean Water
¹¹⁶ (VSMOW).

¹¹⁷ Because precipitation condenses under conditions of equilibrium fractionation, $\delta^{18}O$ and δD in precip-
¹¹⁸ itation evolve along a line with slope c. 8, the global meteoric water line (GMWL) [Voelker et al., 2014].
¹¹⁹ However, kinetic isotope effects associated with differences in diffusivity among the different isotopologues of
¹²⁰ water can lead to deviations from the GMWL [Farquhar et al., 2006]. For example, since $HD^{16}O$ diffusivity
¹²¹ is greater than that of $H_2^{18}O$, the water of a leaf that has undergone heavy transpiration will be more depleted
¹²² in D than in ^{18}O (Fig. 1). Deuterium excess (d-excess) is a widely used measure of how evaporated a pool
¹²³ of water (ocean, lake, leaf) is and is defined as d-excess = $\delta D - 8 \times \delta^{18}O$. The average d-excess for precipi-

¹²⁴ tation is c. 10‰. Lower d-excess values generally indicate that the pool has undergone some evaporation
¹²⁵ [Brooks et al., 2014] (Fig. 1).

¹²⁶ Stable isotopes are also very efficient to identify different water sources in plants [Ehleringer and Dawson, 1992].
¹²⁷ Indeed, simple mixing models allow one to separate the composition and the fluxes coming from differ-
¹²⁸ ent sources [Phillips and Gregg, 2001]. For this reason, stable isotopes are great natural labels that can
¹²⁹ be used to track pathways of water within plants without harming them; they have been the method of
¹³⁰ choice for many studies looking at foliar uptake [Breshears et al., 2008, Limm et al., 2009, Eller et al., 2013,
¹³¹ Berry et al., 2014b]. Indeed, non-meteoric water is usually enriched in heavy isotopes [Scholl et al., 2010],
¹³² making it easy to trace even after entering the leaf.

¹³³ II.2 Experiment 1A: Effects of foliar shielding on leaf isotopes in natural conditions

¹³⁴ Our first experiment examines leaf scale spatial and temporal patterns of water isotopes induced by the
¹³⁵ presence or the absence of dew under natural conditions. Six bulbs of *Colocasia esculenta* were planted in
¹³⁶ separate pots. All pots were placed outside and received full sun for four weeks. During this time, all plants
¹³⁷ were heavily watered with tap water ($\delta^{18}\text{O} \simeq -5.96\text{\textperthousand}$, $\delta\text{D} \simeq -37.63\text{\textperthousand}$) to allow plant growth. Once the six
¹³⁸ plants reached maturity, watering stopped and the plants were moved to a shaded area to remove any sun
¹³⁹ exposure differences between the plants.

¹⁴⁰ Watering stopped two days before the beginning of the treatment. The upper-leaf surfaces in three of
¹⁴¹ the six pots were misted with isotopically-enriched water ($\delta^{18}\text{O} \simeq 8.85\text{\textperthousand}$, $\delta\text{D} \simeq 737.64\text{\textperthousand}$) every two days
¹⁴² using a spray bottle. Any extra water would run off the leaves, leaving them covered in submillimeter-size
¹⁴³ droplets, which is approximately the natural size for dew-deposition drops [Defraeye et al., 2013]. The
¹⁴⁴ misting simulated dew and was always performed around 08:00h.

¹⁴⁵ The three control pots were not watered and did not receive any mist. To avoid contact between the misted
¹⁴⁶ water and the soil in the pots, the surfaces of all pots were covered in wrapping plastic. Six leaves were
¹⁴⁷ collected between the beginning of the control/dew treatments and the end of the experiments, three weeks
¹⁴⁸ later. The sampling and the analysis are described in Section II.5.

149 **II.3 Experiment 1B: Effects of foliar shielding on leaf isotopes under high water stress**

150 Our second experiment was designed to artificially increase the contrast between the control and misted
151 treatments from Experiment 1A. The plants from this former experiment were moved into the laboratory and
152 well watered for multiple weeks to offset any effects from the first experiment. Two leaves of similar size and
153 of the same *Colocasia esculenta* plant were cut at the junction of the petiole and the rachis and left to dry c.
154 80 cm under a blue light (Eiko 1960 EBW, 500 W, 10500 lumens, color temperature of 4800 K). The entire
155 experiment lasted four hours. During that time, the treated leaf was misted with isotopically-labelled water
156 ($\delta^{18}\text{O} \simeq 8.85\text{‰}$, $\delta\text{D} \simeq 737.64\text{‰}$) every half-hour. The control leaf was left to dry without any intervention.
157 After four hours, samples were collected from both leaves as described in Section II.5.

158 **II.4 Experiment 2: Effects of foliar shielding on leaf water potential**

159 In this final experiment, we focused on the effect of water droplet deposition on leaf water potential under
160 high water stressed conditions. One leaf was cut at the junction of the petiole and the rachis and left to dry.
161 Three different water stress conditions were tested here: natural drying (control), high heat drying, and high
162 heat and mist. In the high heat case, the leaf was placed 80 cm under a blue light (Eiko 1960 EBW, 500 W,
163 10500 lumens, color temperature of 4800 K) and left to dry between 8 and up to 10 hours. In the high heat
164 and mist case, the leaf was also misted with ultra pure water every hour using a spray bottle. Again, surplus
165 water was allowed to runoff, leaving the leaf covered in submillimeter size water droplets. Leaf disks of 1 inch
166 diameter were collected every hour, and immediately weighted. The surface of each leaf disk was wetted with
167 ultra pure water, sanded with ultra-fine sandpaper (3M, 600 grit sandpaper), and the water potential analyzed
168 on a WP4C (Decagon Devices Inc.).

169 **II.5 Isotope analysis**

170 For the water isotope analysis, each leaf was sampled in 12 to 25 different locations depending on the size of
171 the leaf. All of the sampling points were located on the same half of the leaf and each point consisted of four

¹⁷² holes (6 mm diameter) punched next to each other forming a square. Each hole was punched as quickly as
¹⁷³ possible to avoid evaporation, which would influence the isotopic composition of the neighboring holes. Each
¹⁷⁴ leaf disk was then secured in an aluminum foil and inserted in a sealed vial. The entire leaf was sampled in
¹⁷⁵ one go. The prepared vials were then stored in the fridge until being analyzed.

¹⁷⁶ The leaf samples were analyzed using an Induction Module (IM) combined to a Cavity Ring Down
¹⁷⁷ Spectrometer (CRDS) L2103-i from Picarro Inc. (Sunnyvale, CA, USA). The IM was set on the ‘normal
¹⁷⁸ leaf’ setting: the leaf disks did not appear carbonized and, after being dried in the oven at 60°C for 48 hours,
¹⁷⁹ they showed no decline in weight, proving that this setting dried the leaf samples completely. The IM was
¹⁸⁰ equipped with a micro-combustion module, which has been proven to efficiently reduce the interferences due
¹⁸¹ to the presence of organics (Kate Dennis, private communication) in water samples extracted from plants
¹⁸² [West et al., 2010]. On average, each half-leaf was sampled in c. 18 different locations, which corresponds to
¹⁸³ c. 73 punched holes.

¹⁸⁴ The entire sampling and IM analysis process lasted from 1.5 to 2 days per half leaf depending on the size
¹⁸⁵ of the leaf, which limited the number of replicas we were able to conduct for this study. However, the number
¹⁸⁶ of leaf disks sampled per leaf far exceeded the c. 25 samples per half leaf collected by [Gan et al., 2002]. In a
¹⁸⁷ different study, [Šantrůček et al., 2007] sampled c. 50 disks per half leaf, but the study was carried out only
¹⁸⁸ in one replicate for each of the two treatments because of time and money constraints. The size of our study
¹⁸⁹ is therefore a significant improvement on previous efforts to map spatial patterns of leaf water isotopes. In
¹⁹⁰ addition, the sampling scheme allowed us to look at the temporal evolution of the spatial patterns, which to
¹⁹¹ the best of our knowledge, had never been done before.

¹⁹² **IM-CRDS analysis sequence** — The IM has only been available commercially for a few years and the
¹⁹³ number of published studies making use of it is still very limited [Berkelhammer et al., 2013]. Here we
¹⁹⁴ present the first detailed protocol for the analysis of leaf samples.

¹⁹⁵ The IM-CRDS analysis sequence was adapted from a protocol developed in [van Geldern and Barth, 2012]
¹⁹⁶ for liquid water samples. Following their notation, Table 1 presents the sequence of standards and samples.

¹⁹⁷ Six empty vials were run at the beginning of each run. The average water vapor content, $\delta^{18}\text{O}$, and δD for
¹⁹⁸ the six vials were measured and introduced in a mixing model that allowed us to retrieve the true isotopic
¹⁹⁹ composition of the sample analyzed. Reference water samples were run using the filter paper provided with
²⁰⁰ the instrument and the same piece of filter paper was reused for all the injections of a single reference water.
²⁰¹ We found that 3 μl of reference water was necessary to reproduce the amount of water contained by one
²⁰² punch hole of *Colocasia esculenta*. The data was corrected for drift and memory effects, and it was also
²⁰³ rescaled back to VSMOW.

²⁰⁴ **IRIS and IRMS analysis** — Ten samples were sent to the Center for Stable Isotope Biogeochemistry
²⁰⁵ at the University of California in Berkeley for IRMS analysis. For the IRMS method, δD was obtained by
²⁰⁶ chromium combustion using an H/Device (Thermo Finnigan, Bremen). Microliters of water were injected
²⁰⁷ in the H/Device and reduced to H_2 gas. The ratio of D/H was then measured on a Thermo Delta Plus mass
²⁰⁸ spectrometer. For the $\delta^{18}\text{O}$ analysis, water from standards and samples were pipetted into glass vials and
²⁰⁹ quickly sealed. The vials were then purged with 0.2% CO_2 in Helium and allowed to equilibrate at room
²¹⁰ temperature for at least 48 hours. The ^{18}O in the CO_2 was then analyzed by continuous flow using a Thermo
²¹¹ Gas Bench II interfaced to a Thermo Delta Plus XL mass spectrometer (Wenbo Yang, private communication).
²¹² In this $\text{H}_2\text{O}-\text{CO}_2$ equilibration method, the dissolved components (organic and/or inorganic) do not affect
²¹³ the values of $\delta^{18}\text{O}$ [West et al., 2010]. For the IRIS analysis, 1.8 μl of water was injected into a vaporizer
²¹⁴ and the vapor was pushed through a MCM with dry air. The concentrations of H_2^{16}O , H_2^{18}O and HD^{16}O were
²¹⁵ measured on a laser spectrometer (L2103-i) from Picarro Inc. (Sunnyvale, CA, USA).

²¹⁶ The ten samples analyzed both by IRMS and IRIS were used to calculate the offset between the two
²¹⁷ techniques. All the samples that had been run exclusively by IRIS or IM-CRDS (and had not been analyzed
²¹⁸ by IRMS) were then corrected for this offset. The IM-CRDS method has not been widely used yet and
²¹⁹ protocols and precision analyses are still absent from the scientific literature. To justify the results from the
²²⁰ IM-CRDS, we compared the values obtained from the extracted water of the half-leaf analyzed by IRIS to the
²²¹ average leaf water composition obtained using a nearest neighbor interpolation on the half-leaf analyzed by

222 IM-CRDS. For the seven leaves analyzed by IM-CRDS, the average difference between those two methods
 223 was $2.6 \pm 0.88\text{\textperthousand}$ in $\delta^{18}\text{O}$ (mean \pm SE) and $3.4 \pm 2.4\text{\textperthousand}$ in δD . One potential source of error comes from the
 224 IM-CRDS analyses being conducted on a different half of a leaf than the IRMS analyses. However, the average
 225 difference we observed between two halves of the same *Colocasia esculenta* leaf was $0.3 \pm 0.2\text{\textperthousand}$ in $\delta^{18}\text{O}$ and
 226 $1.9 \pm 1.2\text{\textperthousand}$ in δD . The differences between the results obtained with the IM-CRDS and the IRMS are therefore
 227 not attributable to the analyses being conducted on different halves of the same leaf. The number of studies
 228 making use of the fast analyzing capacity of the IM-CRDS is slowly growing [Berkelhammer et al., 2013],
 229 but further testing is still clearly necessary before using the IM-CRDS technique as an absolute method.
 230 However, our goal in this present study is to compare strongly enriched water samples and the order of the
 231 differences presented in the next section are up to two orders of magnitude greater than the error observed for
 232 the IM-CRDS. We therefore believe that the IM-CRDS is an appropriate method for our applications.

233 II.6 Linking d-excess and transpiration

234 While d-excess is commonly used in Atmospheric Science [Risi et al., 2013] and for interpreting ice core
 235 data [Luz et al., 2009], it has not been widely used in plant physiology. However, because it combines both
 236 deuterium and ^{18}O , d-excess contains more information than the isotopologues taken separately. Indeed,
 237 lower (more negative) d-excess values are associated with higher transpiration rates [Voelker et al., 2014]. To
 238 interpret d-excess differences in terms of transpiration rates, we link d-excess to steady-state relative humidity.
 239 The steady-state enrichment of leaf water Δ_E above source water is expressed in [Farquhar et al., 2006] as

$$\Delta_E = (1 + \epsilon^*)[(1 + \epsilon_k)(1 - h) + h(1 + \Delta_v)] - 1 \quad (2)$$

240 where h is the relative humidity, ϵ^* is the equilibrium fractionation; $\epsilon^* = 9.2\text{\textperthousand}$ ($74\text{\textperthousand}$) for H_2^{18}O (HDO) at
 241 25°C [Craig and Gordon, 1965]. The kinetic fractionation factor, ϵ_k , is taken as

$$\epsilon_k^{\text{H}_2^{18}\text{O}} = \frac{28.5r_s + 18.9r_b}{r_b + r_s} \quad \text{and} \quad \epsilon_k^{\text{HDO}} = \frac{16r_s + 10r_b}{r_b + r_s} \quad (3)$$

242 for H_2^{18}O and HDO, respectively [Farquhar et al., 1989, Farquhar et al., 2006]. r_s is the stomatal resistance
 243 and it is taken to be constant and equal to 217 s m^{-2} [Hughes et al., 2014]. The resistance of the boundary
 244 layer, r_b , depends on leaf size and wind speed. Here we choose a constant leaf size of 40 cm and a wind
 245 speed of 0.2 m s^{-1} , resulting in an $r_b = 1.13 \cdot 10^5 \text{ s m}^{-2}$. Δ_v is the enrichment of ambient water vapor above
 246 source water, which was calculated for a measured air composition of $\delta^{18}\text{O} = -17\text{\textperthousand}$ and $\delta\text{D} = -100\text{\textperthousand}$.

247 The enrichment relative to a source can be linked back to isotopic compositions expressed in δ notation
 248 through the relative ratios R :

$$\Delta_i = \frac{R_i}{R_{\text{source}}} - 1. \quad (4)$$

249 Using Equation 1 to express R_i as a function of δ_i , we obtain a relation between Δ_i and δ_i

$$\delta_i = \left[\frac{(\Delta_i + 1) R_{\text{source}}}{R_{r_i}} - 1 \right] \times 1000. \quad (5)$$

250 By replacing Δ_i in Equation 5 by its expression from Equation 2 and combining the expressions for $\delta^{18}\text{O}$
 251 and δD , we obtain an expression for the d-excess as a function of the relative humidity h . We solve for h ,
 252 bounding its value between 0 and 1. Assuming that the vapor pressure inside the leaves, e_i , is at saturation,
 253 we may calculate the estimated transpiration rate E (in $\text{mmol m}^{-2} \text{ s}^{-1}$) as

$$E = g_s \frac{e_i^* - h e_{\text{air}}^*}{P}. \quad (6)$$

254 Here, P is the atmospheric pressure taken to be 101.3 kPa and g_s (in $\text{mmol m}^{-2} \text{ s}^{-1}$) is the stomatal conductance
 255 equal to $1/r_s$. e_i^* (in kPa) is the saturated vapor pressure calculated for a leaf temperature of 25°C . e_{air}^* (in
 256 kPa) is the saturated vapor pressure at air temperature, which is also taken to be 25°C . In our analysis, we
 257 compare the transpiration rates of dew treated leaves, E_{dew} , and that of control leaves, E_{control} .

258 **II.7 Spatial patterns**

259 Leaf water isotopic composition is often compared to the isotopic composition of freely evaporating water
260 as described by the Craig-Gordon (CG) model [Craig and Gordon, 1965]. In this model, the fractionation is
261 driven by the difference of saturation vapor pressure between the interior of the leaf and the atmosphere, and
262 by the difference of diffusivity of the isotopologues. However, this simplistic model has been shown to largely
263 underestimate the actual isotopic enrichment. Two main models have since then been proposed to better
264 describe the complexity of leaf water isotopes patterns. The effect of the backward diffusion of enriched
265 water, a form of Péclet effect [Farquhar and Lloyd, 1993, Barbour et al., 2004], has been shown to improve
266 the prediction of bulk water enrichment, as well as the progressive enrichment of leaf water between the xylem
267 and the sites of evaporation [Gan et al., 2002]. The string-of-lakes effect takes into account the progressive
268 enrichment of leaf water along the path of water flow [Yakir et al., 1990, Helliker and Ehleringer, 2000] and
269 improves the modeling of large scale variations of leaf water enrichment.

270 The Craig-Gordon model of evaporation is expressed as [Gan et al., 2002]

$$\Delta_{\text{CG}} = \epsilon_k + \epsilon^* + (\Delta_v - \epsilon_k) \frac{h e_{\text{air}}^*}{e_i^*}, \quad (7)$$

271 with Δ_v the isotopic enrichment of atmospheric water vapor relative to source water (Eq. 4). ϵ_k , r_b , and
272 e_i^* depend on leaf temperature. Using an infrared picture of a *Colocasia esculenta* leaf, we are able to
273 calculate Δ_{CG} at each sampling location that we then compare to the measured isotopic enrichment of leaf
274 water relative to source water (Δ_l , as defined in Eq. 4). Based on meteorologic data available for the duration
275 of the experiment, pressure and relative humidity were taken to be constant and equal to 1013 hPa and 80%,
276 respectively.

277 Because the string-of-lakes and the Péclet models are one-dimensional, they fail to properly represent
278 the true, two-dimensional enrichment of real leaves [Gan et al., 2002]. A two-dimensional model was
279 developed in [Farquhar and Gan, 2003, Gan et al., 2003], but its ability to predict spatial patterns of leaf

280 water enrichment has so far been underused. The Farquhar-Gan (FG) model was initially designed for leaves
 281 with long and disconnected veins, but it has been successful in predicting leaf water enrichment in cotton
 282 leaves [Ripullone et al., 2008]. According to the authors, the aims of the FG model was to take into account
 283 the two-pool model represented by veins and mesophyll water, the effects of the backward diffusion of
 284 enriched water (Péclet effect), and the progressive enrichment along a line of evaporation. Here we use the
 285 expression for a leaf segment [Gan et al., 2003], which includes the weighted effects of lamina and vein water:
 286

$$\frac{\Delta_l}{\Delta_M} = \phi_x \frac{\Delta_x}{\Delta_M} + (1 - \phi_x) \frac{\Delta_{la}}{\Delta_M} \quad (8)$$

287 where ϕ_x is the mass fraction of bulk leaf water coming from the veins. Using eight leaves of *Colocasia*
 288 *esculenta* leaves with lengths ranging from 14 to 64 cm, we determined that $\phi_x = 39.5 \pm 1.2\%$ (mean \pm SE).

289 The ratio of vein water enrichment above source water, Δ_x , over the maximum possible enrichment, Δ_M ,
 290 is given by

$$\frac{\Delta_x}{\Delta_M} = 1 - \frac{{}_1F_1\left[-\frac{k}{2}, \frac{1}{2} - \frac{P_1}{2} \left(1 - \frac{1}{l_m}\right)^2\right]}{{}_1F_1\left[-\frac{k}{2}, \frac{1}{2} - \frac{P_1}{2}\right] + k {}_1F_1\left[1 - \frac{k}{2}, \frac{3}{2} - \frac{P_1}{2}\right]}, \quad (9)$$

291 and the ratio of lamina water enrichment above source water, Δ_{la} , over the maximum possible enrichment,
 292 Δ_M , is described as

$$\frac{\Delta_{la}}{\Delta_M} = 1 - k \left(\frac{e^{P_r}}{h'} - e^{P_r} \frac{1 - e^P}{P} \right) \left(1 - \frac{\Delta_x}{\Delta_M} \right). \quad (10)$$

293 Here, $\frac{1}{l_m}$ is the relative distance from the leaf base, $k = \frac{h'}{e^{P_r} - h'}$ with $h' = 1 - (1 + \epsilon^*)(1 + \epsilon_k)(1 - h)$, and
 294 ${}_1F_1[a, b, y]$ is the Kummer function. P_r , P , and P_l are the total radial, the lamina radial, and the longitudinal
 295 Péclet numbers, respectively. P and P_r can be estimated using the following expressions:

$$\frac{\Delta_b}{\Delta_{CG}^b} = \frac{1 - e^P}{P}, \quad (11)$$

$$\frac{\Delta_b}{\Delta_{CG}^b} = \phi_x e^{-P_r} + (1 - \phi_x) \frac{1 - e^{-\frac{1}{2}P_r}}{\frac{1}{2}P_r}, \quad (12)$$

296 where Δ_b is the isotopic enrichment of bulk leaf water above source water, and Δ_{CG}^b is the Craig-Gordon
297 enrichment of the bulk leaf water above source water.

298 **II.8 Competing effects of foliar uptake and foliar shielding**

299 To compare the relative effects of foliar uptake and foliar shielding, we analyze the results of three different
300 studies that conducted similar experiments on different species. [Limm et al., 2009] looked at a ten different
301 species from the coast redwood ecosystem of California (*Pseudotsuga menziesii* and *Sequoia sempervirens*
302 (conifers), *Polystichum munitum* and *Polystichum californicum* (ferns), *Oxalis oregana* (a short herbaceous),
303 *Arbutus menziesii*, *Gaultheria shallon*, *Vaccinium ovatum*, *Notholithocarpus densiflorus* and *Umbellularia*
304 *californica* (all evergreen broadleaf)), while [Eller et al., 2013] focused on *Drimys brasiliensis*, a woody
305 broadleaf evergreen native from Central and South America, and [Berry and Smith, 2014] concentrated on
306 *Abies fraseri* and *Picea rubens*, two montane conifers from the Appalachian Mountains. All the studies
307 conducted glasshouse experiments in which saplings experienced nighttime fog. Leaf samples were collected
308 in the evening before the fogging treatment and in the morning, right after the treatment. Every study used
309 isotopically labeled fog with a different composition ($\delta D_{fog} - \delta D_{soil} = 16\text{‰}$ in [Berry and Smith, 2014],
310 78‰ in [Limm et al., 2009] and 712‰ in [Eller et al., 2013]). To compare the different experiments, we
311 normalized the results to reflect the leaf water enrichment that would have been observed if the fog water had
312 been 20‰ heavier than soil water, since this is within the range of natural values [Scholl et al., 2010].

313 **II.9 Statistical analysis**

314 Responses for the different experiments were analyzed using a two-sample t-test (Welch's t-test) with a 5%
315 significance level. This test has been recognized as a better alternative to the Student's t-test when dealing
316 with groups of unequal sample size or variance [Ruxton, 2006]. In the following, we will report the p-value,
317 P, the test statistics, t, and the degrees of freedom of the test, v. When comparing the results of the different
318 treatments in Experiments 1A and 1B, we treated the multiple samples collected on each leaf as a single
319 population. stat and syst refer to the statistical and the systematic errors, respectively.

320 III. Results

321 **III.1 Water isotopes**

322 The results of Experiments 1A are presented as maps of the analyzed half leaves (Fig. 2). The maps were
323 obtained using an inverse distance interpolation and show the evolution of the d-excess of leaves from the
324 control and misted treatments collected at 0, 12 (dew), 14 (control) and 21 (dew and control) days from
325 the beginning of the experiment. All the maps of δD and $\delta^{18}O$ (Supporting Information, Fig.s S1 and S2)
326 show a progressive enrichment [Cernusak and Kahmen, 2013] of leaf water when moving away from the
327 main stem towards the rims of the leaf. The average difference between the center and the rim of the leaf for
328 the five leaves presented is $\Delta^{18}O = 11.1 \pm 1.2 \text{‰}$ (mean \pm SE) and $\Delta D = 23.9 \pm 3.3 \text{‰}$. When comparing the
329 composition of the bulk water at the end of the experiment, the dew-treated leaf exhibits a d-excess higher by c.
330 63.0‰ than the control one (two-sample t-test: $t = -9.4$, $v = 29$, $P < 0.001$). There is no statistical difference
331 between the treated and control leaves collected on days 12/14 (difference in mean d-excess $\simeq 10.2 \text{‰}$,
332 two-sample t-test: $t = -1.6$, $v = 35$, $P = 0.11$).

333 Similar maps were produced for Experiment 1B (Fig. 3). In this case, the heat lamp artificially increased
334 the transpiration rate in both the control and the misted leaves, leading to significantly enriched $\delta^{18}O$ and
335 δD values and low d-excess values for both treatments. The d-excess in the control case is c. 173.0‰ more
336 negative than for the dew treated leaves (two-sample t-test: $t = 3.9$, $v = 29$, $P < 0.001$). This experiment was
337 merely an extreme version of Experiment 1A, with the objective of accentuating the contrast between the
338 two treatments. While the high heat treatment led to a strong drying of some areas of the leaf, in particular
339 those far away from the central vein, the significant difference observed between the control and the misted
340 treatments do confirm the results of Experiment 1A.

341 **III.2 Leaf water potential**

342 Experiment 2 looks at the temporal evolution of water potential in artificially drying leaves (Fig. 4). The
343 pressure-volume curve (Fig. 4a) shows a shape characteristic of a high apoplastic fraction [Bartlett et al., 2012].

³⁴⁴ Indeed, *Colocasia esculenta* is known for its high content of mucilage [Quach et al., 2001, Njintang et al., 2014].
³⁴⁵ The polysaccharides constituting the mucilage have been shown to have a large impact on leaf water potential
³⁴⁶ and plant resistance to water-stress [Morse, 1990]: because of their high capacitance (they can hold more
³⁴⁷ than ten times their weight of water), the polysaccharides create a large apoplastic capacitor of available water
³⁴⁸ that can buffer the changes in water potential associated with large variations in leaf water content.

³⁴⁹ Strong differences in drying pattern are shown for the misted and drought leaves (Fig. 4b). In both the
³⁵⁰ control and the high heat and mist cases, the leaf water potential experiences a slow decline, which is well
³⁵¹ approximated by a linear function. However, the high heat treated leaves experience a faster decline and
³⁵² are better approximated by a parabola. Table 2 presents the average decline from initial to final leaf water
³⁵³ potential for the three different treatments. All the data is normalized for leaf size and drying time. The
³⁵⁴ decline in water potential was c. 64% smaller in the misted leaves than in the leaves subjected to the same high
³⁵⁵ heat treatment but that did not get sprayed (two-sample t-test: $t = 2.37, v = 7, P < 0.05$). The decline observed
³⁵⁶ for misted leaves is not statistically different to the one observed for naturally drying leaves (two-sample
³⁵⁷ t-test: $t = -1.46, v = 6, P = 0.19$). [Quach et al., 2001, Njintang et al., 2014]

³⁵⁸ III.3 Foliar shielding-induced decrease in transpiration

³⁵⁹ Treated leaves in Experiments 1A and 1B are all less enriched in heavy isotopes than control ones, despite
³⁶⁰ being sprayed with highly enriched water ($\delta^{18}\text{O} \simeq 8.85\ \text{\textperthousand}$, $\delta\text{D} \simeq 737.64\ \text{\textperthousand}$), which is consistent with a lack
³⁶¹ of foliar uptake. Foliar shielding is then the only phenomenon inducing differences in leaf water d-excess
³⁶² composition between treated and control leaves. We apply the model described in Section II.6 to interpret our
³⁶³ results in terms of the transpiration rate, E .

³⁶⁴ The use of a constant stomatal conductance and leaf temperature are most likely the largest sources
³⁶⁵ of systematic error in this model. To calculate the systematic error associated with our choices for those
³⁶⁶ parameters, we calculate $E_{\text{dew}}/E_{\text{control}}$ for a range of leaf temperatures from 10° to 40°C and for a stomatal
³⁶⁷ conductance g_s from 0.1 to 0.8 $\text{mmol m}^{-2} \text{s}^{-1}$. We find that the systematic error associated with our choice of
³⁶⁸ g_s is negligible, while that associated with the choice of T_{leaf} is important for Experiment 1A, but nor for

369 Experiment 1B.

370 For Experiment 1A, the transpiration rate obtained for the dew treated leaf is significantly lower than that
371 of the control ($t = -9.4$, $\mu = 38$, $P < 0.0001$) by 29.9 ± 2.6 (stat) ± 1.1 (syst) %. Similar results were found for
372 Experiment 1B, where the dew treatment significantly ($t = -3.9$, $\mu = 29$, $P < 0.0001$) decreased transpiration
373 by 29.9 ± 9.1 (stat) %. These values are consistent with [Garratt and Segal, 1988], who estimated that the
374 reduction in transpiration due to dewfall could reduce daily plant water use by c. 10%. This value was
375 obtained for wheat plants associated with a low transpiration rate. Since *Colocasia esculenta* leaves are larger
376 and have a higher transpiration rate, we expect the reduction to be larger in our case (see Section IV.1).

377 **III.4 Spatial patterns**

378 To understand the spatial patterns observed in Figures 2 and 3, we calculate the expected Craig-Gordon
379 (CG) enrichment, Δ_{CG} , for deuterium (Section II.7), and compare the results to the leaf water enrichment
380 above source water, Δ_l (Fig. 5). Leaf water depleted from the expected CG model points toward a larger
381 importance of the Péclet effect, while samples with a ratio Δ_l/Δ_{CG} bigger than 1 show a larger importance of
382 the string-of-lakes effect [Helliker and Ehleringer, 2000, Gan et al., 2002]. Here, we found that neither model
383 is adapted to predict the spatial evolution of leaf water isotopes. However, for the treated leaf of Experiment
384 1A, Δ_l/Δ_{CG} appears to be increasing with distance from the petiole, and we find a strong linear correlation
385 ($R^2 = 0.73$, $P < 0.0005$) between Δ_l/Δ_{CG} and the distance from the petiole (Fig. 5). Similar results are found
386 for the initial leaf ($R^2 = 0.94$, $P < 0.0001$) and the control leaf ($R^2 = 0.79$, $P = 0.0001$) of the same experiment.
387 This pattern of progressive enrichment has already been observed in cotton leaves [Gan et al., 2002] and
388 reflects the failure of the CG model to properly represent leaf water enrichment patterns. Because temperature
389 maps were not available for Experiment 1B, we did not apply the CG model for that case.

390 In order to capture the progressive enrichment of leaf water from petiole to rims, we propose the use
391 of the Farquhar-Gan (FG) model [Farquhar and Gan, 2003, Gan et al., 2003] described in Section II.7. We
392 calculate the laminal radial P and the total radial Péclet number P_r for the dew treated leaf collected at the end
393 of experiment 1A by solving Equations 11 and 12. The bulk leaf water isotopic composition was calculated

394 using the data from the cryogenically-extracted water of the leaves ($\delta^{18}\text{O} \simeq -3.2\text{\textperthousand}$, $\delta\text{D} \simeq 7.5\text{\textperthousand}$), and the
395 bulk CG enrichment is calculated using a relative humidity of 0.86 and an air temperature of 32°C. After
396 replacing Δ_x / Δ_M and Δ_{la} / Δ_M by their expressions from Equations 9 and 10, we solve Equation 8 for P_l (see
397 Fig. 6). The obtained Péclet numbers are the following: $P_r = 0.12$, $P = 0.06$, and $P_l = 0.68$. While the first
398 two numbers are of the same order of magnitude as those reported in [Gan et al., 2003] for maize and wheat,
399 the value of P_l is more than one order of magnitude smaller. As explained in [Gan et al., 2003], lower than
400 expected P_l are most likely associated with extensive longitudinal diffusion in the lamina mesophyll.

401 **Hydraulics of excised leaves** — To verify that the leaf hydraulics of the excised leaves from Experiments
402 1B and 2 are similar to that of the intact leaves of Experiment 1A, we compare the results of the FG model
403 optimized for the intact leaf to the data of a cut leaf (see Fig. 6). In order to take into account the increase
404 in transpiration rate for the leaves in Experiment 1B, the relative humidity is decreased, but all three Péclet
405 numbers are kept constant. We obtain that the model is statistically identical to the data from the excised
406 leaves ($t = -0.95$, $\mu = 30$, $P = 0.34$). The good fit of the adjusted model to the excised leaf data indicates
407 that, while increasing transpiration, sectioning the leaf did not significantly impact the leaf hydraulics itself.
408 Moreover, a thorough comparison of excised and intact leaves of *Lithocarpus edulis* under high evaporative
409 demand [Miyazawa et al., 2011] concluded that the excised leaves had the same photosynthetic rate, stomatal
410 conductance and transpiration rate as the intact leaves for up to 12 hours after being detached. The leaves of
411 *Colocasia esculenta* are much larger than that of *Lithocarpus edulis*, allowing them to buffer the increased
412 water loss from the excision more easily. Moreover, none of our experiments lasted more than 8 hours, most
413 of them lasting only 4 hours. We are therefore confident that the results obtained on excised leaves are a valid
414 representation of the behavior of intact leaves placed in high water-stress conditions.

415 **III.5 Temporal patterns**

416 Leaves collected from both treatments on day 12 or 14 present results that disagree with the trends formed by
417 the results of day 0 and 21 (Fig. 2). It is important to note that the plants were kept outside throughout the

418 experiment and were therefore subjected to the daily variations of temperature and relative humidity, which
419 both influence the transpiration rate as well as the isotopic composition. The dew-treated leaf collected on day
420 12 was sampled after a prolonged period of dry and hot weather that might have enhanced the transpiration
421 despite the artificial dew treatment. This may explain why this leaf presents lower d-excess values than
422 expected. A series of small rain events happened on the day preceding the collection of the first control leaf
423 on day 14, which may have decreased the transpiration rate and increased the d-excess composition of the
424 leaf.

425 IV. Discussion

426 IV.1 Leaf energy cycle

427 Our results show that the deposition of submillimeter size droplets allow the leaf to decrease its transpiration
428 rate and maintain its water potential. The water balance of the leaf is influenced by the change in energy
429 balance associated with the water droplets deposited at the surface through three distinct processes.

430 First, the deposited droplets increase the albedo of the leaf, allowing more of the radiation to be reflected
431 away from the leaf. Depending on the direction of the incoming solar radiation, water can have an albedo as
432 high as 1 (perfect reflector) whereas typical values for leaves are c. 0.2 for visible light. The increase of vegeta-
433 tion albedo due do dew deposition has been observed in the field many times [Pinter, 1986, Zhang et al., 2012].
434 By reflecting more radiation when they are wet, leaves will decrease the incoming shortwave radiation and
435 consequently keep their temperatures lower. This will in turn reduce the evaporative demand and the leaf
436 transpiration. Second, the energy that is not reflected will be dissipated through the evaporation of the
437 droplets. The dissipated energy will not contribute to the leaf energy budget. Moreover, because evapo-
438 ration is an exothermic process, the evaporation of the water droplets will result in a cooling of the leaf
439 surface. This will again reduce the evaporative demand and the transpiration. Finally, the evaporation of
440 the droplets will cause the air close to the leaf to have a higher relative humidity than the surrounding air
441 [Defraeye et al., 2013], creating a moist micro-climate around the leaf [Jones, 1992]. This will decrease

442 the difference between the interstitial and the air vapor pressures, and reduce the flux of water vapor out
443 of the leaf, namely transpiration. By decreasing the outward flow of water vapor, more CO₂ will be able
444 to enter the leaf, increasing interstitial CO₂ concentration, photosynthesis, and water use efficiency. The
445 increase in surface roughness associated with the presence of the droplets at the surface of the leaf will
446 also contribute to increasing the size of the boundary layer. Water potential values are correlated with leaf
447 relative water content [Maxwell and Redmann, 1978] and with stomatal conductance [Lhomme et al., 1998];
448 by maintaining a higher water potential, the leaf will be able to open its stomata wider. CO₂ assimilation is
449 in turn linearly correlated to stomatal conductance [Lambers et al., 2008]. As a result, by affecting the leaf
450 energy cycle, foliar shielding will allow the leaf to maintain its water status and increase CO₂ assimilation
451 through multiple mechanisms.

452 **IV.2 Implications for foliar uptake studies**

453 By decreasing evaporation, foliar shielding suppresses the isotopic enrichment associated with leaf water
454 transpiration [Farquhar et al., 2006]. Therefore, leaves undergoing foliar shielding will have a bulk isotopic
455 composition lower (more depleted) than leaves that do not experience it. The average δD enrichment between
456 the first and last days of collection for Experiment 1A were $-9.1 \pm 3.7 \text{ ‰}$ (mean \pm SE) for the control leaf and
457 $-27.9 \pm 2.9 \text{ ‰}$ for the dew treated leaf. This corresponds to a $-18.8 \pm 6.6 \text{ ‰}$ difference in enrichment between
458 sprayed and control treatments. In the case of highly water stressed leaves (Experiment 1B, Fig. 3), the
459 difference in enrichment reaches $-45.2 \pm 35.8 \text{ ‰}$.

460 Non-meteoric water is usually more enriched in deuterium than rain and soil water by up to 50 ‰
461 [Scholl et al., 2010]. If foliar uptake is indeed happening in a leaf, the uptake of heavy fog water will then
462 enrich the leaf water, while foliar shielding depletes leaf water in heavy isotopes. [Limm et al., 2009] pointed
463 out the tension between foliar uptake and nighttime suppression of respiration due to the saturated atmosphere
464 during fog events. Transpiration is a much larger water loss for plants than respiration and the effects of foliar
465 shielding during day time is expected to be have a even larger impact on leaf isotopes than that discussed by
466 [Limm et al., 2009].

467 Using previous studies on foliar uptake (described in Section II.8), we were able to compare the relative
468 impact of both processes. Foliar uptake has the largest impact on conifers (Fig. 7), where the difference in
469 enrichment between treatment and control reaches up to c. 20 %. Foliar shielding for the non-water stressed
470 case (Experiment 1A) exhibits the opposite effect, with a magnitude similar to the largest foliar uptake case.
471 In the water stressed case (Experiment 1B), the depletion observed is as large as c. 45.2 %. The three foliar
472 experiments presented here all used nighttime treatment, so foliar shielding did not impact the enrichment
473 observed. However, the competing effects of foliar uptake and foliar shielding are likely to be very important
474 when analyzing field or day time foliar uptake experiment data. For example, [Berry et al., 2014b] observed
475 a significantly larger enrichment when fogging saplings in the morning than in the afternoon. This results is
476 well explained if foliar shielding is taken into account, since foliar shielding will have a larger effect in the
477 afternoon, when leaves are hotter and radiations stronger. Our results suggest that, in the field, foliar shielding
478 might have a larger impact on leaf isotopes than foliar uptake.

479 The results of our study show a larger impact of foliar shielding in times of drought than in well-watered
480 conditions. The simultaneous occurrence of non-meteoric water deposition and drought is common in
481 drylands [Agam and Berliner, 2006], where many plants rely on non-meteoric water as their primary source
482 of water [Stanton and Horn, 2013]. Regular dew formation has also been observed in the upper canopy of the
483 Amazon forest during the dry season [Satake and Hanado, 2004, Frolking et al., 2011]. In those cases, the
484 energy balance is thought to be the main driver of leaf water isotopic composition, with a response much
485 larger than to soil water availability, for example [Wayland, 2015]. Foliar shielding will delay the time when
486 leaves reach their maximum transpiration rate and attain isotopic steady state [Dubbert et al., 2014]. Isotopic
487 steady state is often assumed when interpreting transpiration data, but [Dubbert et al., 2013] recently showed
488 that this assumption is typically unjustified and can lead to errors in estimated transpiration fluxes by up to
489 70%, since steady state models systematically overestimate the isotopic enrichment of leaf water. Isotopic
490 steady state depends on the leaf transpiration rate, which changes quickly as energy flux incident on the leaf
491 changes, for example when the leaf goes from the shade to the sun [Smith and Berry, 2013]. Foliar shielding

492 has a large impact at short time scales on both leaf transpiration and water isotopes because of this fast
493 response.

494 **IV.3 Conclusion**

495 In this study, we used the highly hydrophobic leaves of *Colocasia esculenta* to look at the impacts of dew
496 water droplets deposition (called foliar shielding) on the leaf energy, water and isotope balance. We show that
497 simple 1D models fail to properly capture the spatial patterns of leaf water enrichment, and we argue that
498 the two-dimensional Farquhar-Gan model is an appropriate alternative that should be used more extensively.
499 Our results show that foliar shielding significantly decreases leaf transpiration by c. 30%, maintains leaf
500 water potential, and limits leaf water isotopic enrichment. We highlight the opposite effects of foliar uptake,
501 which enriches leaf water in heavy isotopes, and foliar shielding, which depletes it. Because both effects are
502 of similar magnitude, taking both processes into accounts is crucial to properly interpret field data of foliar
503 uptake.

504 **Acknowledgments**

505 The authors thank Todd Dawson and Wenbo Yang for the IRMS analysis, Fulton Rockwell and Missy Holbrook
506 for the discussions on spatial patterns and water potential. C.Gerlein-Safdi and K.K. Caylor acknowledge the
507 financial support of NASA Headquarters under the NASA Earth and Space Science Fellowship Program -
508 Grant 14-EARTH14F-241 - and of the Science, Technology, and Environmental Policy Fellowship from the
509 Princeton Environmental Institute.

REFERENCES

- [Abtew and Melesse, 2012] Abtew, W. and Melesse, A. (2012). *Evaporation and Evapotranspiration - Measurements and Estimations*. Springer Science & Business Media.
- [Agam and Berliner, 2006] Agam, N. and Berliner, P. R. (2006). Dew formation and water vapor adsorption in semi-arid environments—A review. *Journal of Arid Environments*, 65(4):572–590.
- [Allison et al., 1985] Allison, G. B., Gat, J. R., and Leaney, F. W. J. (1985). The relationship between deuterium and oxygen-18 delta values in leaf water. *Chemical Geology: Isotope Geoscience section*, 58(1-2):145–156.
- [Andrade, 2003] Andrade, J. L. (2003). Dew deposition on epiphytic bromeliad leaves: an important event in a Mexican tropical dry deciduous forest. *Journal of Tropical Ecology*, 19(5):479–488.
- [Aryal and Neuner, 2009] Aryal, B. and Neuner, G. (2009). Leaf wettability decreases along an extreme altitudinal gradient. *Oecologia*, 162(1):1–9.
- [Barbour et al., 2004] Barbour, M. M., Roden, J. S., Farquhar, G. D., and Ehleringer, J. R. (2004). Expressing leaf water and cellulose oxygen isotope ratios as enrichment above source water reveals evidence of a Pécelt effect. *Oecologia*, 138(3):426–435.
- [Bartlett et al., 2012] Bartlett, M. K., Scoffoni, C., and Sack, L. (2012). The determinants of leaf turgor loss point and prediction of drought tolerance of species and biomes: a global meta-analysis. *Ecology Letters*, 15(5):393–405.
- [Berkelhammer et al., 2013] Berkelhammer, M., Hu, J., Bailey, A., Noone, D. C., Still, C. J., Barnard, H., Gochis, D., Hsiao, G. S., Rahn, T., and Turnipseed, A. (2013). The nocturnal water cycle in an open-canopy forest. *Journal of Geophysical Research: Atmospheres*, 118(1):10225.

[Berry et al., 2014a] Berry, Z. C., Hughes, N. M., and Smith, W. K. (2014a). Cloud immersion: an important water source for spruce and fir saplings in the southern Appalachian Mountains. *Oecologia*, 174(2):319–326.

[Berry and Smith, 2014] Berry, Z. C. and Smith, W. K. (2014). Experimental cloud immersion and foliar water uptake in saplings of *Abies fraseri* and *Picea rubens*. *Trees*, 28(1):115–123.

[Berry et al., 2014b] Berry, Z. C., White, J. C., and Smith, W. K. (2014b). Foliar uptake, carbon fluxes and water status are affected by the timing of daily fog in saplings from a threatened cloud forest. *Tree Physiology*, 34(5):459–470.

[Breshears et al., 2008] Breshears, D. D., McDowell, N. G., Goddard, K. L., Dayem, K. E., Martens, S. N., Meyer, C. W., and Brown, K. M. (2008). Foliar absorption of intercepted rainfall improves woody plant water status most during drought. *Ecology*, 89(1):41–47.

[Brooks et al., 2014] Brooks, J. R., Gibson, J. J., Birks, S. J., Weber, M. H., Rodecap, K. D., and Stoddard, J. L. (2014). Stable isotope estimates of evaporation: inflow and water residence time for lakes across the United States as a tool for national lake water quality assessments. *Limnology and Oceanography*, 59(6):2150–2165.

[Burgess and Dawson, 2004] Burgess, S. and Dawson, T. E. (2004). The contribution of fog to the water relations of *Sequoia sempervirens* (D. Don): foliar uptake and prevention of dehydration. *Plant, Cell & Environment*, 27(8):1023–1034.

[Cernusak and Kahmen, 2013] Cernusak, L. A. and Kahmen, A. (2013). The multifaceted relationship between leaf water ^{18}O enrichment and transpiration rate. *Plant, Cell & Environment*, 36(7):1239–1241.

[Clus et al., 2008] Clus, O., Ortega, P., Muselli, M., Milimouk, I., and Beysens, D. (2008). Study of dew water collection in humid tropical islands. *Journal of Hydrology*, 361(1-2):159–171.

[Craig and Gordon, 1965] Craig, H. and Gordon, L. I. (1965). Deuterium and oxygen-18 variations in the ocean and the marine atmosphere . *Proceedings of a Conference on Stable Isotopes in Oceanographic Studies and Palaeotemperatures*, pages 9–130.

[Defraeye et al., 2013] Defraeye, T., Verboven, P., Derome, D., Carmeliet, J., and Nicolai, B. (2013). Stomatal transpiration and droplet evaporation on leaf surfaces by a microscale modelling approach. *International Journal of Heat and Mass Transfer*, 65:180–191.

[Dubbert et al., 2013] Dubbert, M., Cuntz, M., Piayda, A., Maguás, C., and Werner, C. (2013). Partitioning evapotranspiration – Testing the Craig and Gordon model with field measurements of oxygen isotope ratios of evaporative fluxes . *Journal of Hydrology*, 496(C):142–153.

[Dubbert et al., 2014] Dubbert, M., Cuntz, M., Piayda, A., and Werner, C. (2014). Oxygen isotope signatures of transpired water vapor: the role of isotopic non-steady-state transpiration under natural conditions. *New Phytologist*, 203(4):1242–1252.

[Ehleringer and Dawson, 1992] Ehleringer, J. R. and Dawson, T. E. (1992). Water uptake by plants: perspectives from stable isotope composition. *Plant, Cell & Environment*, 15(9):1073–1082.

[Eller et al., 2013] Eller, C. B., Lima, A. L., and Oliveira, R. S. (2013). Foliar uptake of fog water and transport belowground alleviates drought effects in the cloud forest tree species, *Drimys brasiliensis*(Winteraceae). *New Phytologist*, 199(1):151–162.

[Evans et al., 1992] Evans, K. J., Nyquist, W. E., and Latin, R. X. (1992). A model based on temperature and leaf wetness duration for establishment of alternaria leaf-blight of muskmelon. *Phytopathology*, 82(8):890–895.

[Farquhar et al., 1989] Farquhar, G., Hubick, K., Condon, A., and Richards, R. (1989). *Stable Isotopes in Ecological Research*, chapter Carbon isotope fractionation and plant water-use efficiency, pages 21–40. Springer New York.

[Farquhar and Lloyd, 1993] Farquhar, G. and Lloyd, J. (1993). *Stable Isotopes and Plant Carbon-water Relations*, chapter Carbon and oxygen isotope effects in the exchange of carbon dioxide between terrestrial plants and the atmosphere, pages 47–70. Academic Press, New York.

[Farquhar et al., 2006] Farquhar, G. D., Cernusak, L. A., and Barnes, B. (2006). Heavy water fractionation during transpiration. *Plant Physiology*, 143(1):11–18.

[Farquhar and Gan, 2003] Farquhar, G. D. and Gan, K. S. (2003). On the progressive enrichment of the oxygen isotopic composition of water along a leaf. *Plant, Cell & Environment*, 26(6):801–819.

[Frolking et al., 2011] Frolking, S., Milliman, T., Palace, M., Wisser, D., Lammers, R., and Fahnestock, M. (2011). Tropical forest backscatter anomaly evident in SeaWinds scatterometer morning overpass data during 2005 drought in Amazonia. *Remote Sensing of Environment*, 115(3):897–907.

[Gan et al., 2003] Gan, K. S., Wong, S. C., and Yong, Jean Wan Hongand Farquhar, G. D. (2003). Evaluation of models of leaf water ^{18}O enrichment using measurements of spatial patterns of vein xylem water, leaf water and dry matter in maize leaves. *Plant, Cell & Environment*, 26(9):1479–1495.

[Gan et al., 2002] Gan, K. S., Wong, S. C., Yong, J. W. H., and Farquhar, G. D. (2002). ^{18}O spatial patterns of vein xylem water, leaf water, and dry matter in cotton leaves. *Plant Physiology*, 130(2):1008–1021.

[Gao and McCarthy, 2006] Gao, L. and McCarthy, T. J. (2006). Contact angle hysteresis explained. *Langmuir*, 22(14):6234–6237.

[Garratt and Segal, 1988] Garratt, J. R. and Segal, M. (1988). On the contribution of atmospheric moisture to dew formation. *Boundary-Layer Meteorology*, 45(3):209–236.

[Gates, 1980] Gates, D. M. (1980). *Biophysical Ecology*. Springer-Verlag, New York.

[Gotsch et al., 2015] Gotsch, S. G., Nadkarni, N., Darby, A., Glunk, A., Mackenzie, D., Davidson, K., and Dawson, T. E. (2015). Life in the Treetops: Ecophysiological Strategies of Canopy Epiphytes in a Tropical Montane Cloud Forest. *Ecological monographs*, 85(3):393–412.

[Griffis et al., 2010] Griffis, T. J., Sargent, S. D., Lee, X., Baker, J. M., Greene, J., Erickson, M., Zhang, X., Billmark, K., Schultz, N., Xiao, W., and Hu, N. (2010). Determining the Oxygen Isotope Composition of Evapotranspiration Using Eddy Covariance. *Boundary-Layer Meteorology*, 137(2):307–326.

[Helliker and Ehleringer, 2000] Helliker, B. R. and Ehleringer, J. R. (2000). Establishing a grassland signature in veins: ^{18}O in the leaf water of C3 and C4 grasses. *PNAS*, 97(14):7894–7898.

[Holder, 2012] Holder, C. D. (2012). The relationship between leaf hydrophobicity, water droplet retention, and leaf angle of common species in a semi-arid region of the western United States. *Agricultural and Forest Meteorology*, 152:11–16.

[Hughes et al., 2014] Hughes, N. M., Carpenter, K. L., Keidel, T. S., Miller, C. N., Waters, M. N., and Smith, W. K. (2014). Photosynthetic costs and benefits of abaxial versus adaxial anthocyanins in *Colocasia esculenta* ‘Mojito’. *Planta*, 240(5):971–981.

[Jones, 1992] Jones, H. G. (1992). *Plants and microclimate: a quantitative approach to environmental plant physiology*. Cambridge University Press.

[Jordan and Smith, 1994] Jordan, D. N. and Smith, W. K. (1994). Energy balance analysis of nighttime leaf temperatures and frost formation in a subalpine environment. *Agricultural and Forest Meteorology*, 71(3):359–372.

[Kabela et al., 2009] Kabela, E. D., Hornbuckle, B. K., Cosh, M. H., Anderson, M. C., and Gleason, M. L. (2009). Dew frequency, duration, amount, and distribution in corn and soybean during SMEX05. *Agricultural and Forest Meteorology*, 149(1):11–24.

[Lakatos et al., 2012] Lakatos, M., Obregón, A., Büdel, B., and Bendix, J. (2012). Midday dew - an overlooked factor enhancing photosynthetic activity of corticolous epiphytes in a wet tropical rain forest. *New Phytologist*, 194(1):245–253.

[Lambers et al., 2008] Lambers, H., Chapin, III, F. S., and Pons, T. L. (2008). *Plant Physiological Ecology*. Springer Science & Business Media.

[Lhomme et al., 1998] Lhomme, J. P., Elguero, E., Chehbouni, A., and Boulet, G. (1998). Stomatal control of transpiration: Examination of Monteith's formulation of canopy resistance. *Water Resources Research*, 34(9):2301–2308.

[Limm and Dawson, 2010] Limm, E. B. and Dawson, T. E. (2010). Polystichum munitum (Dryopteridaceae) varies geographically in its capacity to absorb fog water by foliar uptake within the redwood forest ecosystem. *American Journal of Botany*, 97(7):1121–1128.

[Limm et al., 2009] Limm, E. B., Simonin, K. A., Bothman, A. G., and Dawson, T. E. (2009). Foliar water uptake: a common water acquisition strategy for plants of the redwood forest. *Oecologia*, 161(3):449–459.

[Luz et al., 2009] Luz, B., Barkan, E., Yam, R., and Shemesh, A. (2009). Fractionation of oxygen and hydrogen isotopes in evaporating water. *Geochimica et Cosmochimica Acta*, 73(22):6697–6703.

[Madeira et al., 2002] Madeira, A. C., Kim, K. S., Taylor, S. E., and Gleason, M. L. (2002). A simple cloud-based energy balance model to estimate dew. *Agricultural and Forest Meteorology*, 111(1):55–63.

[Maxwell and Redmann, 1978] Maxwell, J. O. and Redmann, R. E. (1978). Leaf water potential, component potentials and relative water content in a xeric grass, Agropyron dasystachyum (Hook.) Scribn. *Oecologia*, 35(3):277–284.

[Miyazawa et al., 2011] Miyazawa, Y., Tateishi, M., Komatsu, H., Kumagai, T., and Otsuki, K. (2011). Are measurements from excised leaves suitable for modeling diurnal patterns of gas exchange of intact leaves? *Hydrological Processes*, 25(18):2924–2930.

[Monteith, 1963] Monteith, J. (1963). *The Water Relations of Plants*, chapter Dew: Facts and Fallacies. John Wiley & Sons Inc.

[Monteith, 1957] Monteith, J. L. (1957). Dew. *Quarterly Journal of the Royal Meteorological Society*, 83:322–341.

[Mook, 2006] Mook, W. G. (2006). *Introduction to Isotope Hydrology Stable and Radioactive Isotopes of Hydrogen, Carbon and Oxygen*. Taylor & Francis, London.

[Morse, 1990] Morse, S. R. (1990). Water balance in *Hemizonia luzulifolia*: the role of extracellular polysaccharides. *Plant, Cell & Environment*, 13(1):39–48.

[Neinhuis and Barthlott, 1997] Neinhuis, C. and Barthlott, W. (1997). Characterization and distribution of water-repellent, self-cleaning plant surfaces. *Annals of Botany*, 79(6):667–677.

[Njintang et al., 2014] Njintang, N. Y., Boudjeko, T., Tatsadjieu, L. N., Nguema-Ona, E., Scher, J., and Mbafung, C. M. F. (2014). Compositional, spectroscopic and rheological analyses of mucilage isolated from taro (*Colocasia esculenta* L. Schott) corms. *Journal of Food Science and Technology*, 51(5):900–907.

[Phillips and Gregg, 2001] Phillips, D. L. and Gregg, J. W. (2001). Uncertainty in source partitioning using stable isotopes. *Oecologia*, 127(2):171–179.

[Pinter, 1986] Pinter, P. J. (1986). Effect of dew on canopy reflectance and temperature. *Remote Sensing of Environment*, 19(2).

[Proctor, 2012] Proctor, M. C. F. (2012). Dew, where and when? 'There are more things in heaven and earth, Horatio, than are dreamt of in your philosophy...'. *New Phytologist*, 194(1):10–11.

[Quach et al., 2001] Quach, M. L., Melton, L. D., Harris, P. J., Burdon, J. N., and Smith, B. G. (2001). Cell wall compositions of raw and cooked corms of taro (*Colocasia esculenta*). *Journal of the Science of Food and Agriculture*, 81(3):311–318.

[Ripullone et al., 2008] Ripullone, F., Matsuo, N., Stuart-Williams, H., Wong, S. C., Borghetti, M., Tani, M., and Farquhar, G. (2008). Environmental effects on oxygen isotope enrichment of leaf water in cotton leaves. *PLANT PHYSIOLOGY*, 146(2):729–736.

[Risi et al., 2013] Risi, C., Landais, A., Winkler, R., and Vimeux, F. (2013). Can we determine what controls the spatio-temporal distribution of d-excess and ^{17}O -excess in precipitation using the LMDZ general circulation model? *Climate of the Past*, 9(5):2173–2193.

[Rosenzweig and Abramopoulos, 1997] Rosenzweig, C. and Abramopoulos, F. (1997). Land-Surface Model Development for the GISS GCM. *Journal of Climate*, 10(8):2040–2054.

[Rothfuss et al., 2012] Rothfuss, Y., Braud, I., Le Moine, N., Biron, P., Durand, J.-L., Vauclin, M., and Bariac, T. (2012). Factors controlling the isotopic partitioning between soil evaporation and plant transpiration: Assessment using a multi-objective calibration of SiSPAT-Isotope under controlled conditions. *Journal of Hydrology*, 442-443:75–88.

[Ruxton, 2006] Ruxton, G. D. (2006). The unequal variance t-test is an underused alternative to Student's t-test and the Mann-Whitney U test. *Behavioral Ecology*, 17(4):688–690.

[Šantrůček et al., 2007] Šantrůček, J., Kveton, J., Setlík, J., and Bulícková, L. (2007). Spatial variation of deuterium enrichment in bulk water of snowgum leaves. *Plant Physiology*, 143(1):88–97.

[Satake and Hanado, 2004] Satake, M. and Hanado, H. (2004). Diurnal change of Amazon rain forest σ^0 observed by Ku-band spaceborne radar. *IEEE Transactions on Geoscience and Remote Sensing*, 42(6):1127–1134.

[Scholl et al., 2010] Scholl, M., Eugster, W., and Burkard, R. (2010). Understanding the role of fog in forest hydrology: stable isotopes as tools for determining input and partitioning of cloud water in montane forests. *Hydrological Processes*, 25(3):353–366.

[Schreiber and Schönher, 2009] Schreiber, L. and Schönher, J. (2009). *Water and Solute Permeability of Plant Cuticles*. Measurement and Data Analysis. Springer Science & Business Media.

[Smith and Berry, 2013] Smith, W. K. and Berry, Z. C. (2013). Sunflecks? *Tree Physiology*, 33(3):233–237.

- [Stanton and Horn, 2013] Stanton, D. E. and Horn, H. S. (2013). Epiphytes as “filter-drinkers”: life-form changes across a fog gradient. *The Bryologist*, 116(1):34–42.
- [van Geldern and Barth, 2012] van Geldern, R. and Barth, J. A. C. (2012). Optimization of instrument setup and post-run corrections for oxygen and hydrogen stable isotope measurements of water by isotope ratio infrared spectroscopy (IRIS). *Limnology and Oceanography: Methods*, 10:1024–1036.
- [Voelker et al., 2014] Voelker, S. L., Brooks, J. R., Meinzer, F. C., Roden, J., Pazdur, A., Pawelczyk, S., Hartsough, P., Snyder, K., Plavcová, L., and Šantrůček, J. (2014). Reconstructing relative humidity from plant $\delta^{18}\text{O}$ and δD as deuterium deviations from the global meteoric water line. *Ecological Applications*, 24(5):960–975.
- [Vogel, 2012] Vogel, S. (2012). *The Life of a Leaf*. The University of Chicago Press.
- [Wang et al., 2013] Wang, L., Niu, S., Good, S. P., Soderberg, K., McCabe, M. F., Sherry, R. A., Luo, Y., Zhou, X., Xia, J., and Caylor, K. K. (2013). The effect of warming on grassland evapotranspiration partitioning using laser-based isotope monitoring techniques. *Geochimica et Cosmochimica Acta*, 111:28–38.
- [Wayland, 2015] Wayland, H. (2015). An ecohydrological characterization of two African savanna trees under water stress. Master’s thesis, Princeton University.
- [Werner et al., 2012] Werner, C., Schnyder, H., Cuntz, M., Keitel, C., Zeeman, M. J., Dawson, T. E., Badeck, F. W., Brugnoli, E., Ghashghaie, J., Grams, T. E. E., Kayler, Z. E., Lakatos, M., Lee, X., Máguas, C., Ogée, J., Rascher, K. G., Siegwolf, R. T. W., Unger, S., Welker, J., Wingate, L., and Gessler, A. (2012). Progress and challenges in using stable isotopes to trace plant carbon and water relations across scales. *Biogeosciences*, 9(8):3083–3111.
- [West et al., 2010] West, A. G., Goldsmith, G. R., Brooks, P. D., and Dawson, T. E. (2010). Discrepancies between isotope ratio infrared spectroscopy and isotope ratio mass spectrometry for the stable isotope analysis of plant and soil waters. *Rapid Communications in Mass Spectrometry*, 24(14):1948–1954.

- [Wilson et al., 1999] Wilson, T. B., Bland, W. L., and Norman, J. M. (1999). Measurement and simulation of dew accumulation and drying in a potato canopy. *Agricultural and Forest Meteorology*, 93(2):111–119.
- [Yakir et al., 1990] Yakir, D., DeNIRO, M. J., and Gat, J. R. (1990). Natural deuterium and oxygen-18 enrichment in leaf water of cotton plants grown under wet and dry conditions: evidence for water compartmentation and its dynamics. *Plant, Cell & Environment*, 13(1):49–56.
- [Yates and Hutley, 1995] Yates, D. J. and Hutley, L. B. (1995). Foliar Uptake of Water by Wet Leaves of Sloanea woollsii, an Australian Subtropical Rainforest Tree. *Australian Journal of Botany*, 43(2):157–167.
- [Zhang et al., 2012] Zhang, Y.-f., Wang, X.-p., Pan, Y.-x., and Hu, R. (2012). Diurnal and seasonal variations of surface albedo in a spring wheat field of arid lands of Northwestern China. *International journal of Biometeorology*, 57(1):67–73.

Figure Legends

Figure 1: Adapted from [Voelker et al., 2014]: Conceptual figure showing the evaporative conditions controlling the evolution of $\delta^{18}\text{O}$ and δD in leaf water from source water located on the global meteoric water line (GMWL, dashed line). The slope of the transpiration line depends on the relative humidity. The d-excess of a sample is the vertical distance from that sample to the d-excess reference line. The position of the source water along the GMWL depends on the temperature at which the water condensed and on the isotopic composition of the vapor.

Figure 2: Maps of the spacial distribution of d-excess of five *Colocasia esculenta* leaves collected throughout Experiment 1A. The maps were obtained by inverse distance interpolation of 12 to 25 sampling points analyzed on the Picarro Induction Module. All leaves are c. 38 cm long. **Left:** initial leaf collected on day 0. **Top row:** leaves collected on day 14 (center) and 21 (far right) from the control. **Bottom row:** leaves collected on day 12 (center) and 21 (far right) from the sprayed treatment, where the leaves were sprayed with isotopically enriched water ($\delta^{18}\text{O} \simeq 8.85\text{\textperthousand}$, $\delta\text{D} \simeq 737.64\text{\textperthousand}$) every two days. The color scheme is the same for all rows.

Figure 3: Maps of two leaves left to dry under a 500W blue light for four hours. **Top row:** $\delta^{18}\text{O}$, δD and d-excess of the control (not sprayed) leaf. **Bottom row:** $\delta^{18}\text{O}$, δD and d-excess of the leaf sprayed with isotopically enriched water ($\delta^{18}\text{O} \simeq 8.85\text{\textperthousand}$, $\delta\text{D} \simeq 737.64\text{\textperthousand}$) every half-hour. The control leaf shows higher enrichment and lower d-excess values that are associated with enhanced transpiration compared to the sprayed leaf.

Figure 4: Desiccation curves of *Colocasia esculenta* leaves. **(a)** Pressure-volume curve for *Colocasia esculenta*. The shape of the curve is typical characteristic of a high apoplastic fraction [Morse, 1990, Bartlett et al., 2012]. The black line represent a second-order polynomial fit. **(b)** Typical examples of the

temporal evolution of the leaf water potential of *Colocasia esculenta* leaves under three different treatments.

All the leaves under the natural drying (circles) and the high heat and mist (diamonds) treatments are well fit by a linear relation (dotted and dashed lines, respectively). All but one of the leaves under the high heat drying case (squares) are better fit by a parabola (solid line). All the leaves shown here are c. 38 cm long.

Figure 5: Ratio Δ_l/Δ_{CG} for deuterium of the leaf collected on day 21 from the dew treated plant of Experiment 1A as a function of distance l from the petiole relative to leaf total length (l_{max}). Air temperature is set to 30°C, relative humidity to 0.8, and the other parameters are described in Section II.6. The black line represents a linear fit ($R^2 = 0.73$, $P < 0.0005$).

Figure 6: Ratio of lamina enrichment in deuterium over maximum enrichment as a function of distance l from the petiole relative to leaf total length (l_{max}) for an excised (gray circles) and an intact leaf (black triangles). The Farquhar-Gan model was optimized for the intact leaf ($P_r = 0.12$, $P = 0.06$, and $P_l = 0.68$) and is shown for a high relative humidity ($h = 0.86$, solid black line) and a low relative humidity ($h = 0.7$, gray dashed line).

Figure 7: A comparison between the impact of foliar uptake of nighttime fog in three studies [Limm et al., 2009, Eller et al., 2013, Berry and Smith, 2014] to foliar shielding in *Colocasia esculenta*. Bars represent the magnitude of the difference in enrichment between fogged/sprayed and control plants. Enrichment is the difference between pre- and post-treatment leaves. All the foliar uptake data were normalized to reflect enrichment corresponding to a realistic difference of 20 ‰ between rain and fog water [Scholl et al., 2010]. Error bars show one standard error. Because we did not obtain the raw data from the foliar experiments, error bars were not added for those, please refer to the original articles for more details.

Supporting Information

Additional supporting information may be found in the online version of this article.

Figure S1: Interpolated maps showing the δD of the leaves analyzed in Experiment 1A.

Figure S2: Interpolated maps showing the $\delta^{18}O$ of the leaves analyzed in Experiment 1A.

Identifiers		
ID	Type	Injections
Blank 1 to	Empty vial	1
Blank 6	Empty vial	1
DEST	Drift ref. water	10
HIS	High ref. water	10
ANTA	Low ref. water	10
DEST	Drift ref. water	10
HERA	QC ref. water	4
Sample 1 to	Sample	4
Sample 10	Sample	4
DEST	Drift ref. water	6
Sample 11 to	Sample	4
Sample 20	Sample	4
DEST	Drift ref. water	6

Table 1: Typical sequence layout of an IM-CRDS run with four reference waters. Following [van Geldern and Barth, 2012], HIS and ANTA are the names of the reference waters with high and low delta values, respectively. DEST and HERA are intermediate waters. DEST is the drift monitoring reference water, whereas HERA is treated as a sample for quality control. All reference waters except HERA are used for memory and VSMOW correction.

Treatment	Average drop in leaf water potential over 8h (MPa)	SE
Natural drying	0.43	0.03
High heat & mist	1.05	0.31
High heat	2.9	0.77

Table 2: Average drop in water potential (MPa) for the three treatments of Experiment 2: ‘Natural drying’ (control), ‘High heat and mist’ and ‘High heat’. Third column shows one standard error. All the data was normalized to reflect the drop in water potential for a 40 cm long leaf over 8 hours.

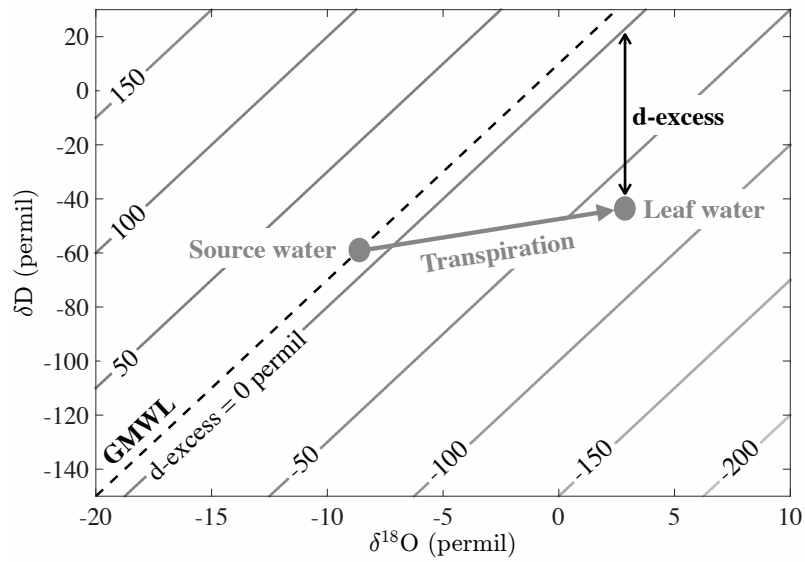


Figure 1

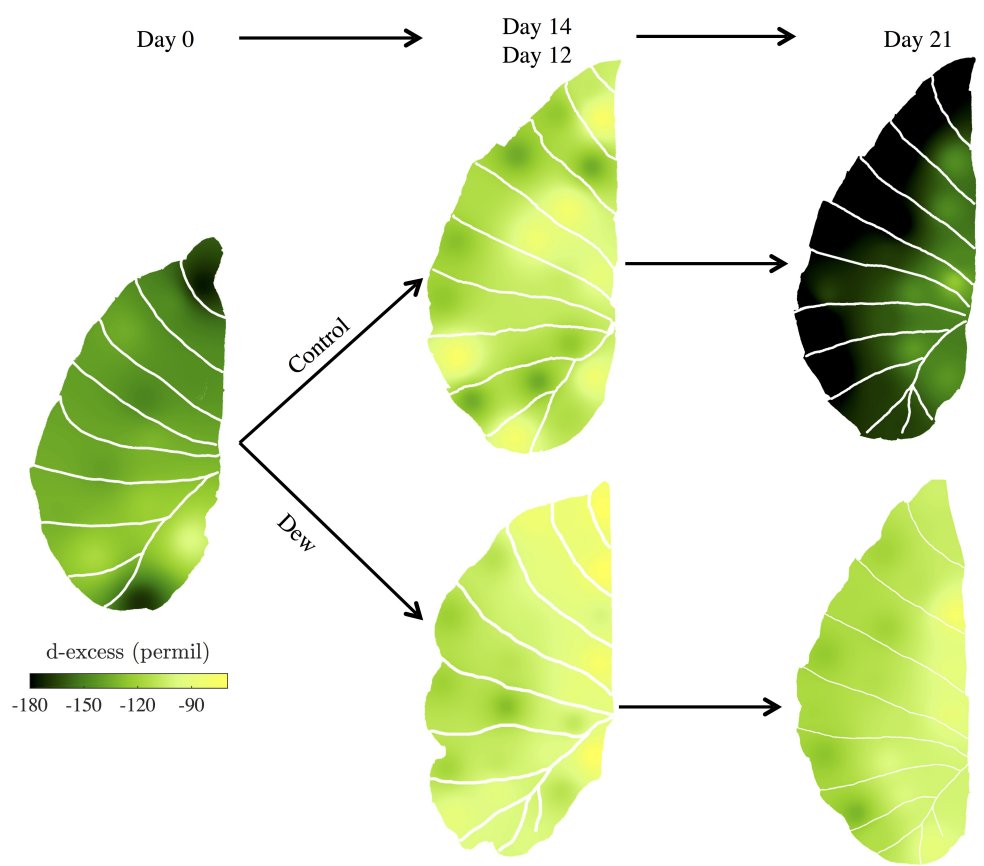


Figure 2

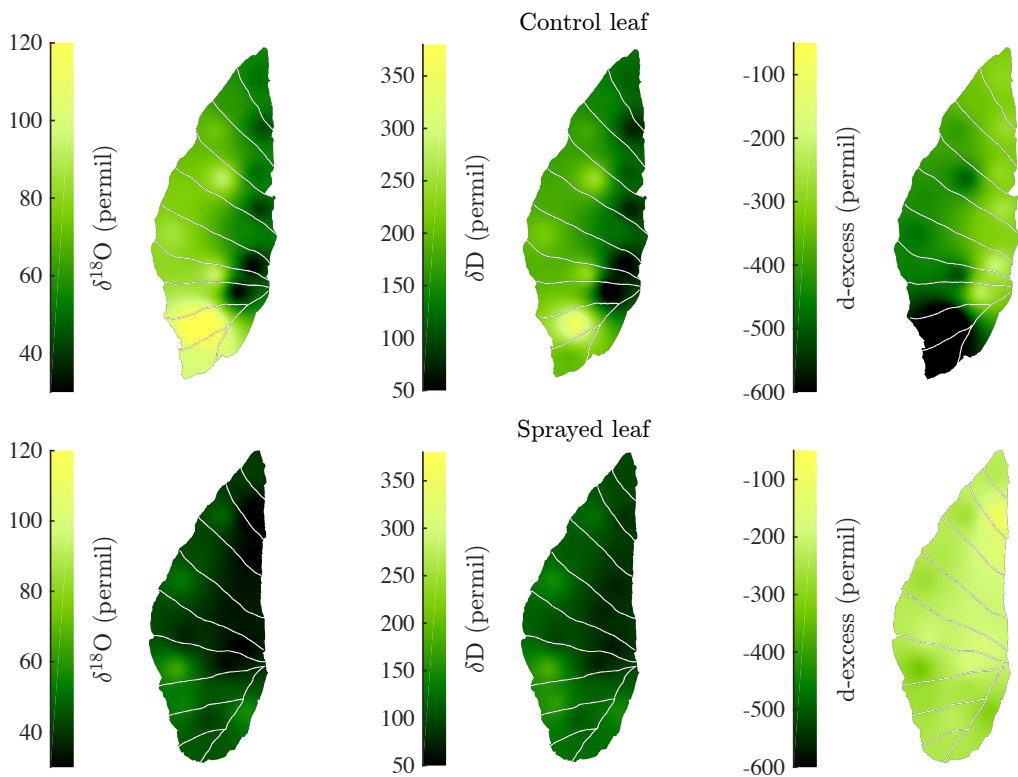


Figure 3

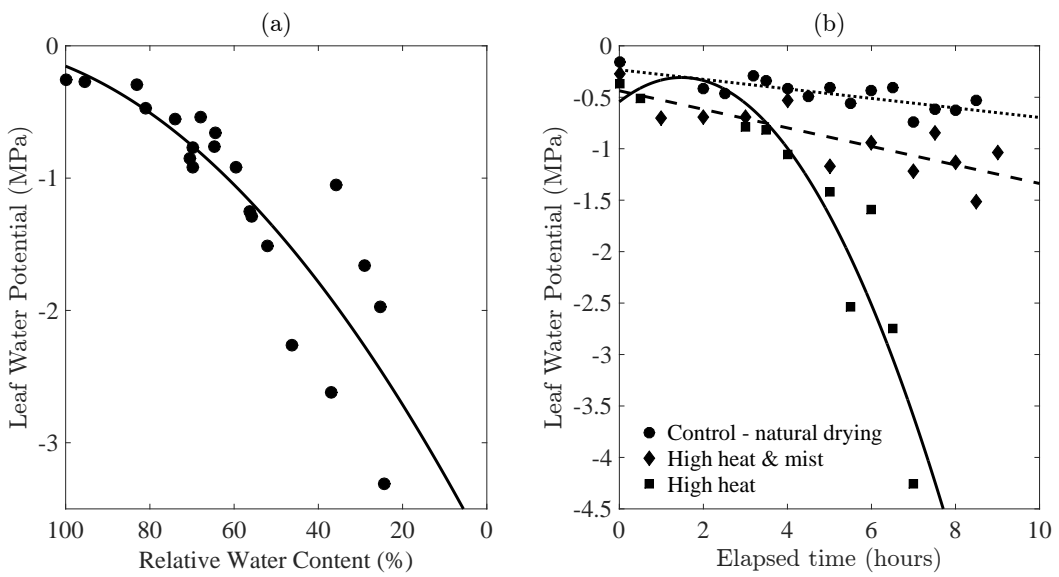


Figure 4

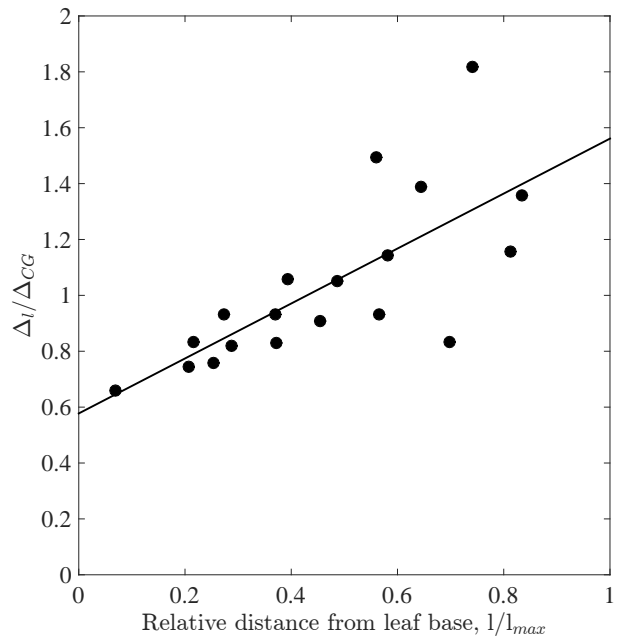


Figure 5

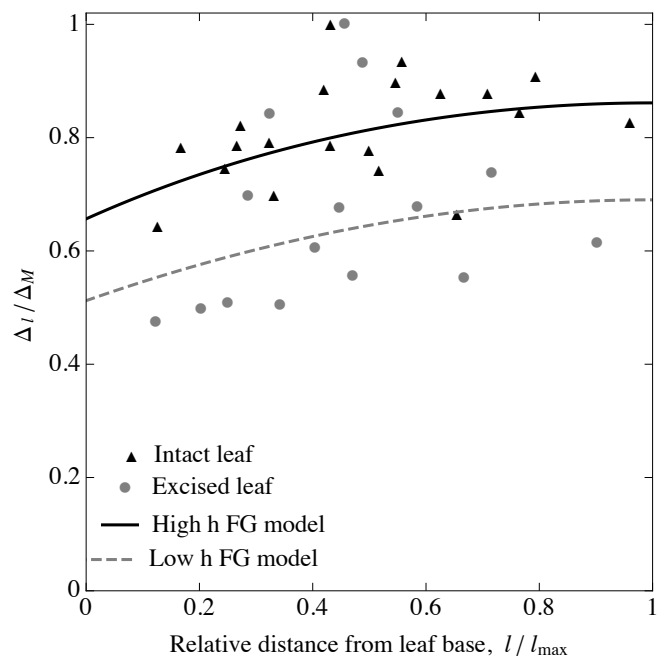


Figure 6

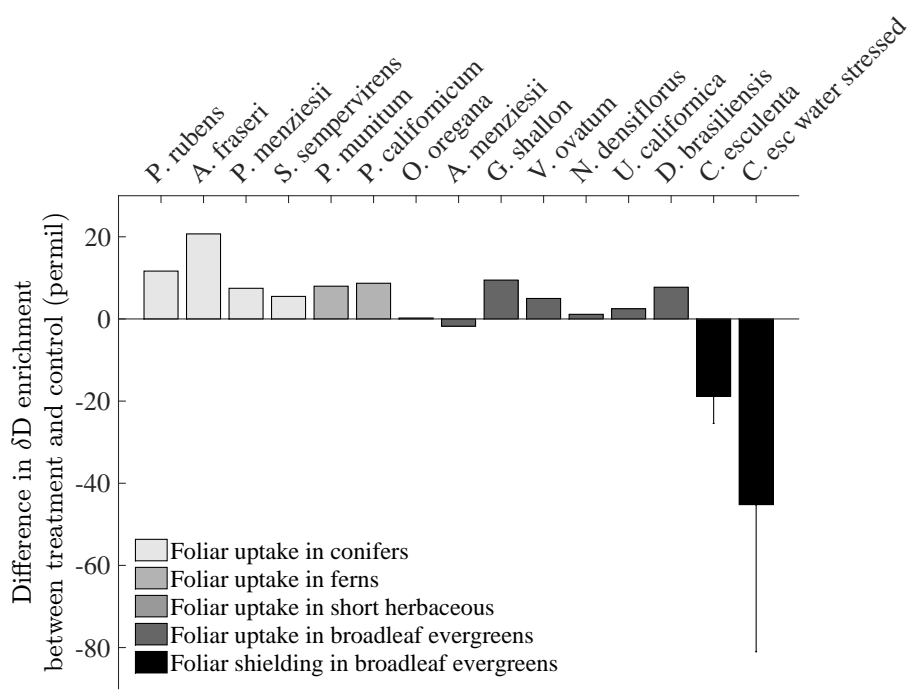


Figure 7

Supplemental Information

Article title: The impacts of dew-induced foliar shielding on the energy, water and isotope balance of leaves

Authors: Cynthia Gerlein-Safdi, Craig James Sinkler, Kelly Krispin Caylor

The following Supporting Information is available for this article:

Fig. S1: Interpolated maps showing the δD of the leaves analyzed in Experiment 1A.

Fig. S2: Interpolated maps showing the $\delta^{18}O$ of the leaves analyzed in Experiment 1A.

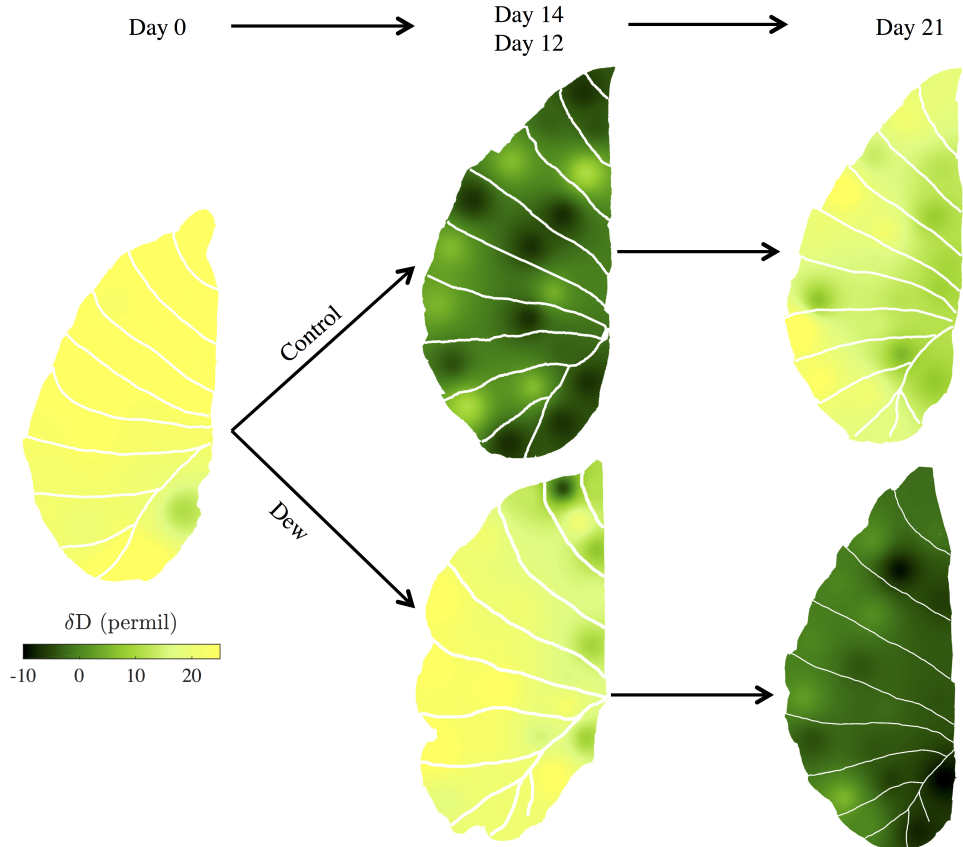


Figure S1: Maps of the spacial distribution of δD of five *Colocasia esculenta* leaves collected throughout Experiment IA. The maps were obtained by inverse distance interpolation of 12 to 25 sampling points analyzed on the Picarro Induction Module. All leaves are c. 38 cm long. **Left:** initial leaf collected on day 0. **Top row:** leaves collected on day 14 (center) and 21 (far right) from the control. **Bottom row:** leaves collected on day 12 (center) and 21 (far right) from the sprayed treatment, where the leaves were sprayed with isotopically enriched water ($\delta^{18}O \approx 8.85\text{‰}$, $\delta D \approx 737.64\text{‰}$) every two days. The color scheme is the same for all rows.

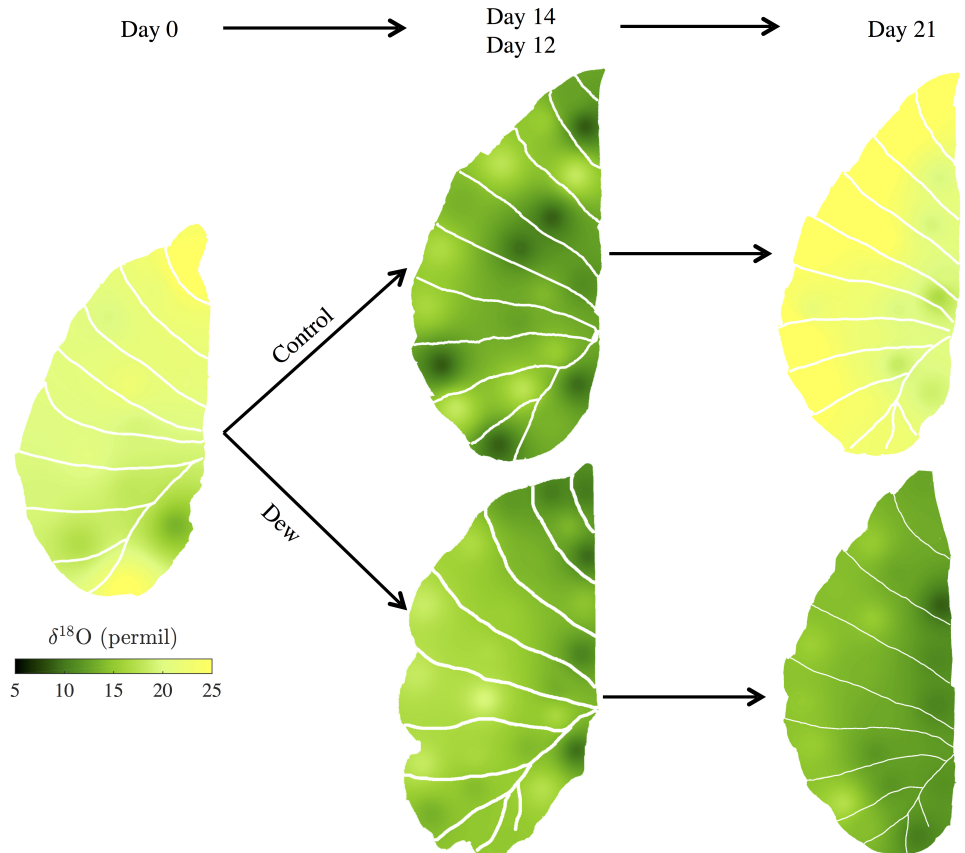


Figure S2: Maps of the spacial distribution of $\delta^{18}\text{O}$ of five *Colocasia esculenta* leaves collected throughout Experiment IA. The maps were obtained by inverse distance interpolation of 12 to 25 sampling points analyzed on the Picarro Induction Module. All leaves are c. 38 cm long. **Left:** initial leaf collected on day 0. **Top row:** leaves collected on day 14 (center) and 21 (far right) from the control. **Bottom row:** leaves collected on day 12 (center) and 21 (far right) from the sprayed treatment, where the leaves were sprayed with isotopically enriched water ($\delta^{18}\text{O} \approx 8.85\text{\textperthousand}$, $\delta D \approx 737.64\text{\textperthousand}$) every two days. The color scheme is the same for all rows.